JOC The Journal of Organic Chemistry

Note

pubs.acs.org/joc

Ethynylene-linked Figure-Eight Octaphyrin(1.2.1.1.1.2.1.1): Synthesis and Characterization of Its Two Oxidation States

Krushna Chandra Sahoo,[†] Marcin A. Majewski,[‡] Marcin Stępień,*[,‡] and Harapriya Rath*[,†]

[†]Department of Inorganic Chemistry, Indian Association for the Cultivation of Science, 2A/2B Raja S. C. Mullick Road, Jadavpur, Kolkata 700032, India

[‡]Wydział Chemii, Uniwersytet Wrocławski, ul. F. Joliot-Curie 14, 50-383 Wrocław, Poland

Supporting Information

ABSTRACT: An octaphyrin(1.2.1.1.1.2.1.1) containing two conjugated ethynylene bridges has been synthesized and characterized. The macrocycle reveals complex conformational dynamics dependent on its protonation and oxidation state. The [40]annulenoid macrocycle and its [38]-annulenoid oxidized form display residual macrocyclic ring currents. In spite of its low apparent aromaticity the new octaphyrin is a potent chromophore with a vis-NIR absorption profile strongly influenced by the redox and acid−base chemistry.

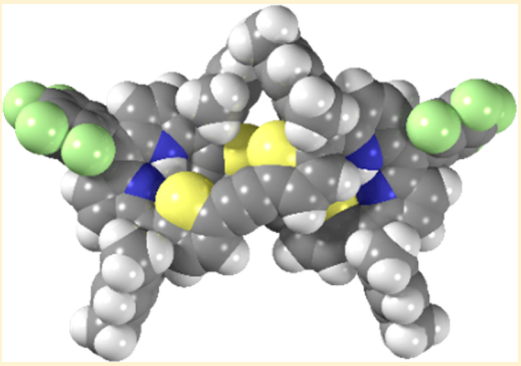

The unusual structural and electronic nature of sp-hybridized carbon contributes to the high current interest in acetylene-containing molecules, spurred not only by theoretical considerations but also by their anticipated applications in nanoelectronics and spintronics, nonlinear optical materials, molecular wires, and other areas.[1] Polyynes containing alternating triple and single bonds are expected to become semiconducting at the carbyne limit while infinite cumulenic chains composed of successive double bonds should exhibit metallic behavior.[2a,b] The acetylene-cumulene dichotomy has driven much of the recent research on polyynes.[2c−e] Simultaneously, the acetylene fragments have played an important role as versatile building blocks, enabling considerable advances in macrocyclic and supramolecular chemistry.[3] In comparison, the chemistry of acetylene-based porphyrinoids has received relatively limited attention.[4] Such hybrid molecules are of particular relevance to aromaticity research, which has flourished through the development of novel expanded porphyrin macrocycles.[5] The ethynylene linkers are longitudinally quite rigid but can simultaneously enable rotational motions, which can lead to restricted conformational freedom and rotational isomerism.[6] Acetylenic linkages can therefore provide a useful means of conformational control,[5] which may become instrumental in the development of porphyrinoid-based molecular switches.

It has been demonstrated that reshuffling of heterocyclic subunits and methine moieties in expanded porphyrins can lead to major structural changes with or without preservation of the main π conjugation pathway, leading to altered physical and chemical properties.[5] Such changes have been documented in a range of octaphyrin-like systems, notably macrocycles **1**−**3** (Chart S1).[7a−d] These observations, complemented by the relative scarcity of acetylene-containing porphyrinoids,[4] provided an incentive to design an expanded ethynylene-bridged porphyrin analogue.

Inspired by our recent work on compound **4**(Chart S1)[7d] which exhibited three distinct π topologies and aromaticity switching, we chose to explore a synthetic design consisting of two dithiatetrapyrrin moieties united by ethynylene linkers (Scheme 1). In the first step of our synthesis, 2-iodothiophene **5** was reacted with trimethylsilylacetylene according to a literature procedure to yield 1,2-di(thiophene-2-yl)ethyne **6**.[8] Further reacting this bithiophene with *n*-butyllithium and mesitaldehyde gave the desired bithiophenediol **7**. In a reaction with pyrrole, catalyzed by trifluoroacetic acid, **7** afforded the hitherto unknown "stretched" tetrapyrrane moiety **8** in quantitative yield.[7d] The synthesis of macrocycle **9** was finally achieved in an acid-catalyzed condensation of **8** with pentafluorobenzaldehyde, followed by oxidation with chloranil.[7d] The best yield was obtained with 0.5 equiv of *p*-toluene sulfonic acid as the catalyst. Column chromatographic separation over basic alumina followed by repeated silica gel (200−400 mesh) chromatographic separation yielded 6% of macrocycle **9** as an air-stable dark green solid.

The new macrocycle was thoroughly characterized via spectroscopic and single-crystal X-ray diffraction analyses. The elemental composition of **9** was confirmed by positive-mode MALDI-TOF mass spectrometry, which showed the parent ion peak at m/z 1516.577. Figure 1A shows UV−vis

Received: July 3, 2017
Published: July 12, 2017

DOI: 10.1021/acs.joc.7b01592
J. Org. Chem. 2017, 82, 8317−8322

Scheme 1. Synthesis of Macrocycle 9 and Its Chemical Oxidation[a]

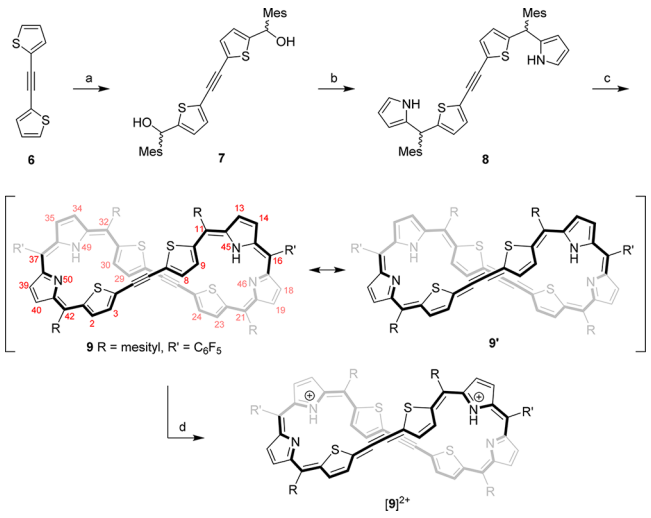

[a]Reagents and conditions: (a) 1. TMEDA, *n*-BuLi, THF; 2. mesitylaldehyde, 67%. (b) pyrrole, TFAH, 57%. (c) 1. C_6F_5CHO, *p*-TsOH, DCM; 2. chloranil, 6%. (d) tris(4-bromophenyl)ammoniumyl hexachloroantimonate (BAHA), dichloromethane (in situ).

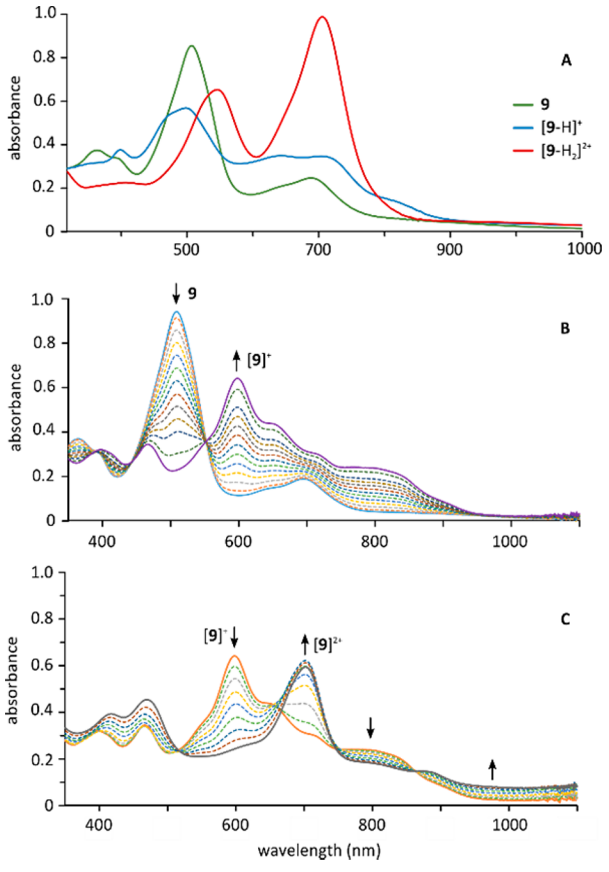

Figure 1. (A) UV−vis absorption spectra of **9** as the free base and upon protonation with TFAH in CH_2Cl_2 at 298 K. (B and C) Changes in the absorption spectrum of **9** observed upon titration with BAHA. The two oxidation stages (**9** to $[\mathbf{9}]^{\cdot+}$ and $[\mathbf{9}]^{\cdot+}$ to $[\mathbf{9}]^{2+}$) are shown separately for clarity.

spectra of the free base and protonated forms of **9**. As the free base, macrocycle **9** exhibits an intense Soret-like band at 509 nm and a broad Q-type absorption that shows a maximum at 700 nm but extends beyond 1000 nm. The latter feature indicates a relatively narrow optical band gap, potentially corresponding to an antiaromatic system.[9] Titration of **9** with trifluoroacetic acid resulted in two consecutive protonation events with well-resolved isosbestic points (Figure S11). Upon second protonation, **9** exhibits two intense bands at 546 and 708 nm and low intensity Q-like band in the 900−1200 nm region.

Single crystals suitable for X-ray diffraction were obtained by slow diffusion of petroleum ether into a dichloromethane solution of **9**. In the free base form (Figure S35), the macrocycle turned out to have a figure-eight conformation (denoted A) with the figure-eight "twisted Hückel" topology.[5f] The four thiophene rings were found to adopt two different orientations ("regular" vs "inverted"[5f]) relative to the adjacent pyrrolic rings, leading to a decrease of effective molecular symmetry to C_2. The ethynylene C≡C distances were 1.190(6) and 1.217(6) Å, whereas the lengths of adjoining C−C bonds were in the 1.40−1.41 Å range. These structural features are consistent with the DFT-optimized geometry of **9** (e.g., 1.214 Å for the ethynylene), indicating good localization of the triple bonds in the macrocycle and essentially acetylenic, rather than cumulenic conjugation. With the CCC angles of 178 to 179°, the ethynylene bridges in **9** are almost perfectly linear, suggesting that the figure-eight conformation observed in the crystal is relatively unstrained.

The ^{1}H NMR spectra of **9** provided detailed insight into the conformational flexibility of the macrocycle (Figure S14). At 300 K in CD_2Cl_2, the ^{1}H NMR spectrum of the free base form contains one pair of *β*-pyrrolic signals (6.33 and 6.13 ppm), one pair of broadened *β*-thiophene signals (7.40 and 7.00 ppm), one set of signals corresponding to the mesityl group (with two methyl peaks at 2.11 and 2.44 ppm in a 2:1 intensity ratio), and a single peak at 12.06 ppm, corresponding to pyrrole NHs. These spectral features are consistent with the maximum attainable symmetry of the molecular framework (apparent D_{2h}), indicating rapid NH tautomerism and in view of the observed broadened lines, a dynamically averaged conformation. Indeed, gradual lowering of the temperature resulted in further line broadening and eventually led to a well-resolved spectrum corresponding to a stationary conformer with an effective C_2 symmetry. Spectral assignment made at 220 K on the basis of 2D data was in very good agreement with calculated GIAO shifts (Figure S29) and confirmed that the conformation of **9** in solution is a figure-eight structure of type A, analogous to that observed in the solid state for **9**. In the free base **9**, the pyrrolic NHs are localized opposite the "non-inverted" thiophene rings, as represented in Scheme 1.

Titrations of **9** with trifluoroacetic acid (TFAH) in CD_2Cl_2, performed at low temperatures under ^{1}H NMR control revealed the formation of well-defined protonated forms, monocation $[\mathbf{9}\text{-H}]^+$ and dication $[\mathbf{9}\text{-H}_2]^{2+}$. In the presence of 0.5 equiv TFAH, an equilibrium mixture of **9** and $[\mathbf{9}\text{-H}]^+$ (A-type conformer) was observed at 190 K (Figures S21−S23). Under these conditions, intermolecular proton transfer processes involving the three species were too slow to be observed by ROESY. The conformation of $[\mathbf{9}\text{-H}]^+$ was found to be similar to that of **9**. At 230 K, the monocation revealed an EXSY pattern consistent with an untwisting motion of the figure-eight macrocycle, but no proton transfer between the two nonequivalent half-cavities was observed (Figure S24). The behavior of the dication was more complex and depended on

DOI: 10.1021/acs.joc.7b01592
J. Org. Chem. 2017, 82, 8317−8322

the concentration of excess acid. At 220 K, the spectrum was heavily broadened during initial titrations steps, and a well resolved set of signals was only formed at ca. 4 equiv of added acid. Interestingly, the observed spectral pattern corresponded to apparent D_{2h} symmetry, as in the room-temperature spectrum of the freebase **9**. Splitting of the *o*-Me signal could be induced by addition of 50 equiv of TFAH at 220 K, whereas decoalescence to a spectrum of lower symmetry (probably C_2) was observed at 170 K in the presence of 20 equiv TFAH. Unexpectedly, in addition to the major form of $[\mathbf{9}\text{-}H_2]^{2+}$ described above (A), and additional doubly protonated species (X) was observed at high acid concentrations. The X species was characterized by a spectrum with D_{2h}-like symmetry, with narrow lines that did not broaden with the addition of acid. The population of the X form increased both with the acid concentration and the temperature, reaching ca. 9% at 260 K and 50 equiv TFAH. Under these conditions no exchange between A and X was observable by ROESY (Figure S25).

DFT calculations indicated that there was no stationary conformation available for $[\mathbf{9}\text{-}H_2]^{2+}$ that would be characterized by complete planarity of the macrocycle, as implied by the D_{2h} symmetry of the X species observed in solution. Instead, a range of nonplanar conformers were identified computationally, including two D_2-type figure eight structures (B and C, cf. Figure S31), and a C_{2h}-symmetric nontwisted form (D, Figure S32). This result indicated that the X species is most likely undergoing rapid conformational averaging under the conditions of the NMR experiment. With all thiophene S atoms pointing inward, the B form (Figure S31) is the only one that should not yield an NH−*β*-thiophene dipolar contact in the ROESY spectrum, as indeed experimentally observed for X. On this basis, B was selected as the most probable geometry of the X conformer. In DFT calculations, the B−D conformers were determined to have higher energies than the corresponding A structures of **9** and $[\mathbf{9}\text{-}H_2]^{2+}$ (ca. 5 to 13 kcal/mol). It should however be noted that the X species is stabilized by addition of excess TFA, an effect that could not be reliably modeled by DFT. In partial support of the above assignment, the calculated relative energy ΔE_{B-A} actually decreases on going from **9** to $[\mathbf{9}\text{-}H_2]^{2+}$ (from 12.96 to 8.15 kcal/mol), in opposition to the corresponding changes of ΔE_{C-A} and ΔE_{D-A} differences.

The above spectral data along with DFT calculations provide support for the conformational behavior of **9** summarized in Scheme S2. The lower-symmetry conformation A is prevalent for all protonation levels and is rapidly equilibrating at room temperature. At low temperatures, the equilibration is markedly faster for the dication than for the less protonated forms, but it can be somewhat slowed down with the addition of a large acid excess. The X = B form is stabilized by the interaction with excess trifluoroacetic acid and is thus only observed for the dication.

9 contains a [40]annulenoid conjugation pathway, formally antiaromatic, which can be represented with two Kekulé-type valence structures, acetylene-like **9** and cumulene-like **9′** (Scheme 1). ^{1}H NMR shifts of peripheral *β*-H protons in **9**, $[\mathbf{9}\text{-}H]^+$, and $[\mathbf{9}\text{-}H_2]^{2+}$-A are in the range characteristic of nonaromatic porphyrinoids (6.0 to 7.5 ppm), with the exception of the "inner" thiophene signal, which appears above 8.0 ppm. In $[\mathbf{9}\text{-}H_2]^{2+}$-B, *β*-H protons resonate in the 6.1 to 5.7 ppm range, which, together with the more downfield shift of the NH protons (12.09 ppm vs 9.43 ppm in $[\mathbf{9}\text{-}H_2]^{2+}$-A), may indicate a residual paratropic current. It should be noted that the weakness of ring currents was also noticeable in figure-eight 41,43,45,47-tetrathia[*n*]octaphyrins(1.1.1.1.1.1.1.1) (*n* = 36, 38; compound **2** in Chart S1), which may be seen as smaller homologues of **9**.[7b] These conclusions are further supported by NICS calculations performed for A and B conformations of $[\mathbf{9}\text{-}H_2]^{2+}$ (Table S2),which reveal moderate diatropicity of constituent pyrrole and thiophene rings and a weak paratropic ring current inside the macrocycle (NICS(0) of ca. 3 to 4 ppm at the center of each dithiatetrapyrrin fragment).

Electronic properties of the new macrocycle were further probed with cyclic voltammetry and differential pulse voltammetry in dichloromethane using 0.1 M tetrabutylammonium hexafluorophosphate as a supporting electrolyte. Compound **9** exhibits two reversible oxidation waves at 0.48 and 0.64 V, followed by two quasi-reversible oxidations at 1.24 and 1.42 V (Figure S33). An irreversible reduction peak was detected at ca. −0.92 V, yielding an estimate of the electrochemical HOMO−LUMO gap (HLG) of 1.40 V. As expected of an expanded porphyrinoid, the latter value is considerably reduced relative to *meso*-tetraphenylporphyrin (2.26 V),[10] although it is still larger than the optical HLG of **9**, derived from its electronic spectrum, which is apparently smaller than 1.2 eV.

Titration of **9** with tris(4-bromophenyl)ammoniumyl hexachloroantimonate (BAHA), a powerful one-electron oxidant, was followed spectrophotometrically in dichloromethane. It was found that **9** undergoes two well-separated oxidation steps, which, on the basis of electrochemistry data, were proposed to involve the formation of radical cation $[\mathbf{9}]^{\cdot+}$ and dication $[\mathbf{9}]^{2+}$. This assumption was further confirmed by the initial disappearance of signals observed in ^{1}H NMR-spectroscopic titration monitored at 220 K (Figure S26). This behavior was consistent with the formation of a paramagnetic species, i.e., a radical cation. Subsequent addition of BAHA resulted in the emergence of a single species yielding a sharp, well-resolved NMR spectrum ascribed to the dicationic product $[\mathbf{9}]^{2+}$.

The chemical oxidation of **9** involves a striking color change from red, through blue, to green−yellow, which reflected the rise of new bands in the visible range of the spectrum (Figure 1B). Additionally, an overall increase of near-infrared absorption was observed for the consecutive oxidized forms (Figure 1C). The oxidized dication $[\mathbf{9}]^{2+}$ was found to be a relatively short-lived species in solution and it decomposed to unidentified products over the course of several hours at room temperature. These products could not be reverted to the neutral **9** by treatment with zinc powder, which caused only further bleaching of the solution. Nevertheless the dication was sufficiently stable at 220 K in CD_2Cl_2, to permit its characterization using 2D NMR spectroscopy (Figures S27, S28). It was found that $[\mathbf{9}]^{2+}$ exhibits a conformational dichotomy similar, though not identical, to that seen for the protonated dication $[\mathbf{9}\text{-}H_2]^{2+}$. At 220 K, the major conformer of $[\mathbf{9}]^{2+}$ displays a C_2-symmetric spectral pattern corresponding to the A-type conformation. It is accompanied by a minor, D_2-symmetric conformer (molar ratio 4 to 1 at 220 K). In the ROESY spectrum recorded at 200 K, the latter species revealed a strong dipolar correlation between the inner NHs and one of the thiophene *β* positions, consistent with quadruple thiophene ring inversion, i.e., a C- or D-type conformation. DFT calculations strongly support the figure-eight conformation of type C (Figure S31), which is predicted to be thermally accessible (ΔE_{C-A} = 1.76 kcal/mol).

DOI: 10.1021/acs.joc.7b01592
J. Org. Chem. 2017, 82, 8317−8322

According to the conventional electron count,[5f] $[9]^{2+}$ is a [38]annulenoid system and is thus expected to reveal macrocyclic aromaticity. However, as previously found for **9**, the observed ^{1}H NMR spectral patterns of the two conformers indicated that the macrocyclic ring current is very weak. Residual diatropicity might be the cause of the observed shielding of the most upfield thiophene signals of $[9]^{2+}$-A and $[9]^{2+}$-C, which resonate respectively at 6.03 and 4.86 ppm. In partial support of this conjecture, moderately negative dithiapyrrane NICS(0) values of −1.55 and −6.89 ppm, respectively, were determined for the two conformers. Interestingly, the DFT optimized geometries of $[9]^{2+}$-A and $[9]^{2+}$-C show geometrical nonequivalence of ethynylene units. In each conformer, the bond length pattern in one of the units shows a noticeable cumulenic contribution (Figure S30), consistent with partial π-bond localization in the macrocycle, according to the valence structure shown in Scheme 1.

In conclusion, we have presented here a concise and efficient synthesis of an acetylene-containing octaphyrin derivative. This new system shows borderline aromaticity characteristics and drastic changes of its optical signatures upon protonation and chemical oxidation. The latter processes have been shown to switch on conformational equilibria between differently twisted geometries of the large and partially flexible porphyrinoid ring. We believe that further studies of such expanded macrocycles may lead to development of functional electrochromic switches and sensors.

EXPERIMENTAL SECTION

Materials and Methods. Electronic absorption spectra were measured using a UV−vis-NIR spectrophotometer, and variable temperature UV−vis-NIR were carried out in a cryostat. ^{1}H, and ^{13}C NMR spectra were recorded on a spectrometer (operating as 600.17 MHz for ^{1}H and 150.91 MHz for ^{13}C) using the residual solvents as the internal references for ^{1}H [($CHCl_3$ (δ = 7.26 ppm), CH_2Cl_2 (δ = 5.32 ppm). MALDI-TOF MS data were recorded using Bruker Daltonics flex Analyzer and ESI HR-MS data were recorded using Waters QTOF Micro YA263 spectrometer. Cyclic voltammograms were recorded using a platinum working electrode, a platinum wire counter electrode and an Ag/AgCl reference electrode in Bioanalytical Systems EC epsilon. The measurements were carried out in CH_2Cl_2 solution using 0.1 M Bu_4NPF_6 as the supporting electrolyte at a scan rate of 0.1 V/s. Peak potentials were determined from differential pulse voltammetry experiments. The Fc/Fc^+ redox couple was used as an internal standard. All solvents and chemicals were of reagent grade quality, obtained commercially and used without further purification except as noted. For spectral measurements, anhydrous dichloromethane was obtained by refluxing and distillation over CaH_2. Dry THF was obtained by refluxing and distillation over pressed sodium metal. Thin layer chromatography (TLC) was carried out on alumina sheets coated with silica gel 60 F_{254} and gravity column chromatography were performed using silica gel 230−400 mesh.

X-ray Structure Determination. A suitable shining blue crystal of size suitable shinning green crystal of size 0.19 × 0.18 × 0.18 mm^3 of free base **9** was mounted on a Bruker APEX-II CCD diffractometer with a fine- focus sealed tube Mo Kα (λ = 0.71073 Å) X-ray source. Total 1800 frames were collected at 100 K for free base form of **9** with the exposure time of 20 s per frame. Unit cell determination using both high angle and low angle diffraction reveal that compound crystallizes in triclinic $P-1$ space group for **9**. The structures were solved by SHELX- 2016/4 using SHELXTL suite of program. The final refinement of the structure was carried out using least-squares method on F^2 using SHELXL-2016/4. The final refinement of the solved structure converged at the R value of 0.0888 ($I > 2\sigma(I)$) for free base form of **9**. All non-hydrogen atoms were refined anisotropically. All the hydrogen atoms were located from difference Fourier maps. Crystal quality was good, however we could not fix solvent molecules due to having potential disorder. We tried fixing H for solvent molecules but it is going for NPD. Hence, we left it without fixing H for solvent molecules.

Computational Chemistry. Density functional theory (DFT) calculations were performed using Gaussian 09 (see ref S1 in the SI). DFT geometry optimizations were carried out in unconstrained C_1 symmetry, using molecular mechanics or semiempirical models as starting geometries. DFT calculations were performed using either the dispersion-corrected ωB97XD functional (see ref S2 in the SI) (general optimizations), the B3LYP functional (see refs S3−S5 in the SI) (NICS calculations, in vacuo) or the KMLYP functional (see ref S6 in the SI) (^{1}H GIAO shifts, in vacuo), each combined with the 6-31G(d,p) basis set. For each functional, DFT geometries were refined to meet standard convergence criteria and the existence of a local minimum was verified by a normal-mode frequency calculation. Nucleus-Independent Chemical Shift (NICS) calculations (see refs S7,S8 in the SI) were performed with gas-phase calculated GIAO shieldings.

SYNTHESIS

2-(2-(Thiophen-2-yl)ethynyl)thiophene (6). To an oven-dried 25 mL round-bottom flask were added $Pd(PPh_3)_2Cl_2$ (67.4 mg, 6 mol%), CuI (30.5 mg, 10 mol%), and 2-iodothiophene (0.17 mL, 1.6 mmol), and the flask was purged with argon. Argon-purged anhydrous toluene (8 mL) and DBU (1.43 mL, 6 equiv) were added successively by syringe. Ice-chilled trimethylsilylethyne (104.5 μL, 0.50 equiv) was then added by syringe, followed immediately by distilled water (11.5 μL, 40 mol%). The reaction flask was covered by aluminum foil and stirred for 18 h at RT. Then the reaction mixture was partitioned in ethyl ether and distilled water (50 mL each). The organic layer was washed with 10% HCl (3 × 75 mL) and saturated aqueous NaCl (75 mL) and dried over $MgSO_4$. The crude product was purified by silica gel column chromatography using ethyl acetate−hexane (0.1:99.9) solution.

Yield: 130.9 mg, 86%, Mp 98 °C. ^{1}H NMR (400 MHz, $CDCl_3$) δ 7.27−7.31 (m, 4H), 7.00−7.02 (m, 2H). ^{13}C NMR (100 MHz, $CDCl_3$) δ 132.2, 127.7, 127.2, 123.0, 86.3. HR-ESI-TOF MS (m/z): Found 189.9951 $[M]^+$ (Calcd189.9911. for $[C_{10}H_6S_2]^+$). Elemental analysis: Calcd for $C_{10}H_6S_2$: C, 63.12; H, 3.18.; S, 33.7. Found: C, 63.14; H, 3.16; S, 33.72.

2,5-Bis(mesitylhydroxymethyl)-1,2-Di(thiophen-2-yl)-ethyne (7). To a 250 mL round-bottomed flask equipped with a magnetic bar, **6** (1.354 g, 7.13 mmol) was placed followed by dry THF (40 mL). The reaction mixture was stirred under inert atmosphere. N, N, N′, N′-Tetramethyl ethylenediamine (3.2 mL, 0.021 mol) was added followed by stirring for half an hour at room temperature. Afterward, n-BuLi in hexane (1.6 M) (13.04 mL, 0.021 mol) was added through rubber septa dropwise, yellow turbidity started forming. The reaction mixture was stirred at room temperature for 2 h and then heated to 66 °C for 1 h. The reaction mixture was brought to room temperature after which it was brought to ice cold temperature. At ice cold temperature, mesitaldehyde (2.62 mL, 0.017 mol) in dry THF (40 mL) was then added dropwise to the reaction mixture, the reaction mixture was stirred for 2 h. The reaction mixture was quenched by saturated NH_4Cl (aq) solution, product was extracted by diethyl ether, dried over Na_2SO_4. The crude product was precipitated out by hexane and purified by silica gel column chromatography using the mixture of ethyl acetate−hexane (20:80) solution. The solvent was evaporated and light yellow solid was obtained.

Yield 2.30gm (67%). Mp 135 °C. ^{1}H NMR (500 MHz, CDCl3, 300 K, δ [ppm]): 1.65 (brs, 2H); 2.28(s, 6H); 2.31(s,

DOI: 10.1021/acs.joc.7b01592
J. Org. Chem. 2017, 82, 8317−8322

12H); 6.39(s, 2H); 6.52(d, 2H, J = 3.5 Hz); 6.86 (s, 4H); 7.05 (d, 2H, J= 3.5 Hz). ^{13}C NMR (125 MHz, $CDCl_3$, 300 K, δ [ppm]): 20.3, 20.8, 69.3, 86.4, 122.2, 123.5, 130.0, 131.9, 135.3, 136.7, 137.8, 150.2. HR-ESI-TOF MS (m/z): Found 509.0054 $[M+Na]^+$ (Calcd 509.1585 for $[C_{30}H_{30}O_2S_2\ Na]^+$). Elemental analysis: Calcd for $C_{30}H_{30}O_2S_2$: C, 74.04; H, 6.21.; O, 6.57.; S, 13.18. Found: C, 74.10; H, 6.48; O, 6.30.; S, 13.20.

2-(Mesityl(1H-pyrrole-2-yl)methyl) 1,2-Di(thiophen-2-yl)ethyne-5-yl)methyl)-1H-pyrrole (8). Compound 7 (1.11 g, 2.29 mmol) was dissolved in pyrrole (15 mL, 0.19 mol). The solution was stirred for 45 min under nitrogen atmosphere at room temperature. Trifluoroacetic acid (0.05 mL, 0.22 mmol) was added and stirred for 1 h. The reaction mixture was quenched by dichloromethane; product was neutralized by NaOH (aq) solution, extracted by dichloromethane, dried over Na_2SO_4, and dried in rotary evaporator to give yellow oil. The crude product was purified by silica gel chromatography using ethyl acetate−hexane (10:90) solution. Compound **8** was obtained as light yellow foam. Yield 0.760 g (57%). ^{1}H NMR (500 MHz,$CDCl_3$, 300 K, δ [ppm]): 2.11(s, 12H,-Me); 2.28(s, 6H, -Me); 6.06(s, 2H,-CH); 6.13(brs, 2H, β-H of pyrrole); 6.17(s, 2H, β-H of pyrrole); 6.66(d, 2H, J = 4.5, β-H of pyrrole); 6.74(d, 2H, J = 4.5, β-H of thiophene); 6.87 (s, 4H, −CH); 7.06 (d, 2H, β-H of thiophene); 7.84(brs, 2H, -NH). ^{13}C NMR (125 MHz, $CDCl_3$, 300 K, δ [ppm]): 20.7, 40.6, 86.2, 107.0, 108.5, 116.5, 121.4, 125.6, 130.4, 131.4, 131.6, 135.2, 136.9, 137.3, 148.2. HR-ESI-TOF MS (m/z): Found 584.7821$[M^+]$ (Calcd 584.23 for $[C_{38}H_{36}N_2S_2]^+$). Elemental analysis: Calcd for $C_{38}H_{36}N_2S_2$: C, 78.04; H, 6.20.; N, 4.79.; S, 10.97. Found: C, 78.20; H, 6.25; N, 4.85.; S, 10.97.

General Synthetic Procedure for Compound 9. Under nitrogen atmosphere and in dark condition, a solution of 584 mg of compound **8** (1 mmol) and pentafluorobenzaldehyde (0.12 mL, 1 mmol) in 250 mL dry dichloromethane was stirred for 30 min. Afterward, catalytic amount of p-TSA (95 mg) was added to the reaction mixture and stirred at RT for 90 min. Then chloranil (490 mg, 1.99 mmol) was added and opened to air and the mixture was refluxed for another 1 h. The solvent was removed under reduced pressure and compound was filtered by basic alumina followed by repeated silica gel column chromatography with the mixture of dichloromethane−hexane (40:60) solution. After recrystallization, the title compound was obtained as dark-red crystals. Yield. ∼ 91 mg (∼6%). Mp > 300 °C MALDI-TOF MS (m/z): 1516.57 (Calc. 1516.37 for $[C_{90}H_{62}F_{10}N_4S_4]^+$). Elemental analysis: Calcd for $C_{90}H_{62}F_{10}N_4S_4$: C, 71.22; H, 4.12.; F, 12.52.; N, 3.69.; S, 8.45. Found: C, 71.38; H, 4.15; F, 12.39.; N, 3.74.; S, 8.44. UV−vis (CH_2Cl_2, λ [nm], (ϵ [M^{-1} $cm^{-1}\times10^3$]), 298 K): 508(43.79); 700 (8.56). [(UV−vis [CH_2Cl_2, 1% TFA/CH_2Cl_2, λ [nm], (ϵ [M^{-1} $cm^{-1}\times10^3$]), 298 K)]: 546 (34.40); 708 (56.86), 900−1200 (stretched band).

■ ASSOCIATED CONTENT

Supporting Information

The Supporting Information is available free of charge on the ACS Publications website at DOI: 10.1021/acs.joc.7b01592.

X-ray crystallographic data for compound **9** (CIF)

Jmole files (ZIP)

Scheme, conformational dynamics of **9** at different protonation level, HR-ESI-TOF mass spectra, MALDI-TOF mass spectra, NMR spectra (^{1}H NMR, ^{13}C NMR, acid titration, variable temperature, ^{1}H−^{1}H COSY, ^{1}H−^{1}H ROESY, ^{1}H−^{1}H NOESY), details of absorption spectroscopic (acid titration, variable temperature study), results of DFT calculations, X-ray crystallographic details. (PDF)

■ AUTHOR INFORMATION

Corresponding Authors

*marcin.stepien@chem.uni.wroc.pl

*ichr@iacs.res.in

ORCID

Marcin Stępień: 0000-0002-4670-8093

Harapriya Rath: 0000-0002-5507-5275

Notes

The authors declare no competing financial interest.

■ ACKNOWLEDGMENTS

K.C.S. thanks CSIR, New Delhi for senior research fellowship. H.R. thanks DST-SERB (EMR/2016/004705), New Delhi, India for research grant. Financial support from the National Science Center of Poland is kindly acknowledged (DEC-2012/07/E/ST5/00781 to M.S.). Quantum-chemical calculations were performed in the Centers for Networking and Supercomputing of Wrocław and Poznań. Our sincere thanks to Dr. P. Sasikumar, Presidency University, Kolkata, India for final refinement of crystal data reported in the manuscript.

■ REFERENCES

(1) (a) Liu, M.; Artyukhov, V. I.; Lee, H.; Xu, F.; Yakobson, B. I. *ACS Nano* **2013**, *7*, 10075. (b) Eisler, S.; Slepkov, A. D.; Elliott, E.; Luu, T.; McDonald, R.; Hegmann, F. A.; Tykwinski, R. R. *J. Am. Chem. Soc.* **2005**, *127*, 2666. (c) Kminek, I.; Klimovic, J.; Prasad, P. N. *Chem. Mater.* **1993**, *5*, 357. (d) Moreno-Garcia, P.; Gulcur, M.; Manrique, D. Z.; Pope, T.; Hong, W.; Kaliginedi, V.; Huang, C.; Batsanov, A. S.; Bryce, M. R.; Lambert, C.; Wandlowski, T. *J. Am. Chem. Soc.* **2013**, *135*, 12228.

(2) (a) Milani; Lucotti, A.; Russo, V.; Tommasini, M.; Cataldo, F.; Li Bassi, A.; Casari, C. S. *J. Phys. Chem. C* **2011**, *115*, 12836. (b) Weimer, M.; Hieringer, W.; Della Sala, F.; Gorling, A. *Chem. Phys.* **2005**, *309*, 77. (c) Szafert, S.; Gladysz, J. A. *Chem. Rev.* **2003**, *103*, 4175. (d) Szafert, S.; Gladysz, J. A. *Chem. Rev.* **2006**, *106*, PR1. (e) Januszewski, J. A.; Tykwinski, R. R. *Chem. Soc. Rev.* **2014**, *43*, 3184.

(3) (a) Zhang, W.; Moore, J. S. *Angew. Chem., Int. Ed.* **2006**, *45* (27), 4416−4439. (b) Kawase, T.; Kurata, H. *Chem. Rev.* **2006**, *106* (12), 5250−5273. (c) Stępień, M.; Gońka, E.; Żyła, M.; Sprutta, N. *Chem. Rev.* **2017**, *117* (4), 3479−3716.

(4) (a) Jux, N.; Koch, P.; Schmickler, H.; Lex, J.; Vogel, E. *Angew. Chem., Int. Ed. Engl.* **1990**, *29*, 1385. (b) Martire, D. O.; Jux, N.; Aramendia, P. F.; Negri, R. M.; Lex, J.; Braslavsky, S. E.; Schaffner, K.; Vogel, E. *J. Am. Chem. Soc.* **1992**, *114*, 9969. (c) Anderson, S.; Anderson, H. L.; Sanders, J. K. M. *Acc. Chem. Res.* **1993**, *26*, 469. (d) Ueta, K.; Naoda, K.; Ooi, S.; Tanaka, T.; Osuka, A. *Angew. Chem., Int. Ed.* **2017**, *56*, 7223.

(5) (a) Sessler, J. L.; Weghorn, S. J. *Expanded, Contracted and Isomeric Porphyrins*; Pergamon: New York, 1997; Vol *15*, p 429. (b) Chandrashekar, T. K.; Venkatraman, S. *Acc. Chem. Res.* **2003**, *36*, 676. (c) Chatterjee, T.; Srinivasan, A.; Ravikanth, M.; Chandrashekar, T. K. *Chem. Rev.* **2017**, *117*, 3329. (d) Sessler, J. L.; Seidel, D. *Angew. Chem., Int. Ed.* **2003**, *42*, 5134. (e) Tanaka, T.; Osuka, A. *Chem. Rev.* **2017**, *117*, 2584. (f) Stępień, M.; Sprutta, N.; Latos-Grażyński, L. *Angew. Chem., Int. Ed.* **2011**, *50*, 4288. (g) Sung, Y. M.; Yoon, M.-C.; Lim, J. M.; Rath, H.; Naoda, K.; Osuka, A.; Kim, D. *Nat. Chem.* **2015**, *7*, 418. (h) Sung, Y. M.; Oh, J.; Cha, W.-Y.; Kim, W.; Lim, J. M.; Yoon, M.-C.; Kim, D. *Chem. Rev.* **2017**, *117*, 2257.

(6) Toyota, S. *Chem. Rev.* **2010**, *110*, 5398.

DOI: 10.1021/acs.joc.7b01592
J. Org. Chem. 2017, 82, 8317−8322

(7) (a) Shin, J.-Y.; Furuta, H.; Yoza, K.; Igar-ashi, S.; Osuka, A. *J. Am. Chem. Soc.* **2001**, *123*, 7190. (b) Sprutta, N.; Latos-Grażyński, L. *Chem. - Eur. J.* **2001**, *7*, 5099. (c) Karthik, G.; Lim, J. M.; Srinivasan, A.; Suresh, C. H.; Kim, D.; Chandrashekar, T. K. *Chem. - Eur. J.* **2013**, *19*, 17011. (d) Mallick, A.; Oh, J.; Majewski, M.; Stępień, M.; Kim, D.; Rath, H. *J. Org. Chem.* **2017**, *82*, 556.
(8) Mio, M. J.; Kopel, L. C.; Braun, J. B.; Gadzikwa, T. L.; Hull, K. L.; Brisbois, R. G.; Markworth, C. J.; Grieco, P. A. *Org. Lett.* **2002**, *4* (19), 3199.
(9) Shin, J.-Y.; Yoon, M.-C.; Lim, J. M.; Yoon, Z. S.; Osuka, A.; Kim, D.; Kim, K. S. *Chem. Soc. Rev.* **2010**, *39*, 2751.
(10) Kadish, K. M. *Prog. Inog.Chem.* **1986**, *34*, 435.

DOI: 10.1021/acs.joc.7b01592
J. Org. Chem. 2017, 82, 8317−8322